



Photoactivation of sulfonated polyplexes enables localized gene silencing by DsiRNA in breast cancer cells

Anu Puri, PhD^{a,*}, Mathias Viard, PhD^{a,b}, Paul Zakrevsky, PhD^a, Serena Zampino^a,
Arabella Chen^a, Camryn Isemann^a, Sohaib Alvi, BS^a, Jeff Clogston, PhD^{b,c},
Upendra Chitgupi, PhD^d, Jonathan F. Lovell, PhD^d, Bruce A. Shapiro, PhD^{a,*}

^aRNA Structure and Design Section, RNA Biology Laboratory, National Cancer Institute, Frederick, MD, USA

^bBasic Science Program, Frederick National Laboratory for Cancer Research, Frederick, MD, USA

^cNanotechnology Characterization Lab, Frederick National Laboratory for Cancer Research, Frederick, MD, USA

^dDepartment of Biomedical Engineering, University at Buffalo, The State University of New York, Buffalo, NY, USA

Revised 23 January 2020

Abstract

Translation potential of RNA interference nanotherapeutics remains challenging due to *in vivo* off-target effects and poor endosomal escape. Here, we developed novel polyplexes for controlled intracellular delivery of dicer substrate siRNA, using a light activation approach. Sulfonated polyethylenimines covalently linked to pyropheophorbide- α for photoactivation and bearing modified amines (*sulfo*-pyro-PEI) for regulated endosomal escape were investigated. Gene knock-down by the polymer-complexed DsiRNA duplexes (siRNA-NPs) was monitored in breast cancer cells. Surprisingly, *sulfo*-pyro-PEI/siRNA-NPs failed to downregulate the PLK1 or eGFP proteins. However, photoactivation of these cell associated-polyplexes with a 661-nm laser clearly restored knock-down of both proteins. In contrast, protein down-regulation by *non*-sulfonated pyro-PEI/siRNA-NPs occurred without any laser treatments, indicating cytoplasmic disposition of DsiRNA followed a common intracellular release mechanism. Therefore, sulfonated pyro-PEI holds potential as a unique *trap and release* light-controlled delivery platform for on-demand gene silencing bearing minimal off target effects.

Key words: RNA interference; siRNA delivery; Polymer; Photosensitizer; Endosomal escape

RNA interference (RNAi) is a biological phenomenon that modulates gene expression and significantly impacts cellular processes.¹ Various small non-coding RNAs such as small interfering RNAs (siRNAs), microRNAs (miRNAs), short hairpin RNAs (shRNAs), and piwi-interacting RNAs (piRNAs) have been demonstrated to initiate the process of RNAi.² Research is underway to develop RNA-based therapeutics that

exploit RNAi for the treatment of diseases such as infections,³ cancer⁴, cardiovascular diseases,⁵ and eye-related disorders.^{6,7} RNAi-based therapies can be applied either on their own merit or in combination with other drugs.^{8–10}

Most widely studied RNAi-therapeutics utilize siRNAs as the molecules of choice with several clinical trials currently in the pipeline.^{11,12} siRNAs are generally constructed as a ~21 base

Abbreviations: FBS, Fetal bovine serum; DMEM, Dulbecco's Modified Eagle Medium supplemented with 10% (v/v) heat-inactivated FBS, 100 i.u./mL penicillin and 100 μ g/mL streptomycin; HBSS+, Hanks' balanced salt solution supplemented with Ca²⁺ & Mg²⁺ ions; BSA, Bovine serum albumin; EEA1, early endosomal antigen 1 (ThermoFisher Inc. cat # PA1-063A); PBS, Phosphate buffered saline (2.66 mM KCl, 1.47 mM KH₂PO₄, 138 mM NaCl, 8.06 mM Na₂HPO₄-7H₂O) (pH 7.1); Nucleic Acid Assembly buffer, 2 mM Mg(OAc)₂, 50 mM KCl, 89 mM Tris, 89mM boric acid (pH 8.2); HEPES buffer (HBS), 10 mM HEPES, 140 mM NaCl (pH 7.2-7.5); TBE buffer, 89 mM Tris, 89 mM boric acid, 2 mM EDTA (pH 8.2); ROS, Reactive oxygen species; RIPA, Radio immunoprecipitation assay

REVISED Manuscript Pyro-PEI mediated DsiRNA release

This research was supported in part by the Intramural Research Program of the NIH, National Cancer Institute, Center for Cancer Research. This project has been funded in whole or in part with federal funds from the National Cancer Institute, National Institutes of Health, under contract HHSN261200800001E. The content of this publication does not necessarily reflect the views or policies of the Department of Health and Human Services, nor does mention of trade names, commercial products, or organizations imply endorsement by the U.S. Government.

This research was supported by the National Institutes of Health (R01EB017270 and DP5OD017898), the National Science Foundation (1555220) and the University at Buffalo Clinical and Translational Science Institute.

*Corresponding authors at: RNA Biology Laboratory, National Cancer Institute, Frederick, MD, 21202, USA.

E-mail addresses: puria@mail.nih.gov (A. Puri), shapirbr@mail.nih.gov (B.A. Shapiro).

<https://doi.org/10.1016/j.nano.2020.102176>

1549-9634/Published by Elsevier Inc.

pair (bp) duplex with 2 nucleotide 3'-overhangs. Cellular pathways obligatory for biological function of siRNAs have been identified and thus provide strategies for their intended therapeutic intervention. Alternatively, slightly longer RNA duplexes (25-30 bp), termed Dicer substrate interfering RNAs (DsiRNAs), can be employed to accomplish gene silencing. DsiRNAs require intracellular processing by the ribonuclease-III enzyme Dicer before loading into the RISC complex.^{13,14} DsiRNAs display superior gene silencing compared to siRNAs in general, and can be designed to induce polarity in the nucleic acid duplexes that may determine which strand of the duplex ultimately becomes the guide strand.^{13,14}

Intracellular delivery of siRNA in its functional form can be achieved by using chemically modified siRNAs or self-assembled RNA nanostructures with multiple functionalities.^{15,16} An alternative approach utilizes selected delivery agents to carry the unmodified siRNAs to their desired site(s).^{17,18} Among these, cationic lipids are widely studied, and various lipid-based delivery systems have entered clinical trials for systemic delivery of siRNA.^{9,19} The first lipid-based RNAi therapeutic (patisiran, ONPATTRO) was approved by the FDA for the treatment of Polyneuropathy of Hereditary Transthyretin-Mediated Amyloidosis (Alnylam Pharmaceuticals, Inc. Cambridge, MA). Cationic polymers are another class of widely studied molecules to deliver siRNA due to their inherent positively-charged surfaces for siRNA binding.²⁰⁻²³

RNAi nanotherapeutics can either enter cells by direct cytosolic delivery of the siRNA^{24,25} or the particles can be endocytosed. However, the RNAi activity of endocytosed nanoparticles is often hindered due to the lack of efficient and directed cytoplasmic siRNA disposition.^{26,27} Therefore, suitable strategies for endosomal/lysosomal escape of siRNA for controlled, spatial and temporal release are vital for efficient RNAi.²⁸ In the field of small molecule drug-loaded nanomedicine, ample literature exists describing stimuli sensitive nanoparticles with their clinical manifestations.³³⁻³⁶ However, only limited research has been done in the field of stimuli-sensitive siRNA nanomedicine.^{31,34} A few tunable siRNA-nanoparticles (siRNA-NPs, often referred as triggerable NPs) responsive to pH²⁹, redox potential,²⁹ heat,³⁰ and photoactivation^{31,32} have been reported. Ideally, a tunable nanosystem should have the following features: (i) minimum or no gene silencing prior to triggering (no off-target effects), (ii) reasonable gene silencing *only* upon triggering, and (iii) translational potential of the technology for patient care.

Here, we aimed to develop photoactivatable polymer-based RNA nanoparticles to accomplish controlled cytoplasmic DsiRNA release upon treatment with a suitable light source. Our design parameters include (i) selection of a photosensitive molecule that can be activated by a tissue-penetrating wavelength with preferred biological activity of its own, (ii) incorporation of this agent into a positively charged nanoformulation without impeding subsequent interactions with the DsiRNA, (iii) minimal effects of light treatments on the biological function of DsiRNA as well as on the cell viability, and (iv) preferential uptake of the nanoparticles *via* an endocytic mechanism for regulated cytoplasmic release of DsiRNA.

Differential uptake of aromatic, sulfonic acid-modified nanoparticles by endothelial cells has been reported earlier.³⁷

In addition, the affinity of sulfonated molecules for cell-surface expressed adhesion molecules (such as Selectins) has been documented.³⁸ In view of these indications, we previously developed sulfonated polyethylenimine polymers (*sulfo*-PEI). These modified PEI were covalently linked to a far-red photodynamic therapy molecule, pyropheophorbide- α (pyro) and hence designated as *sulfo*-pyro-PEI.³⁹ The parent non-sulfonated photoreactive polymer, designated as pyro-PEI, was used for comparison purposes. These sulfonated polymers that retained their binding activity with DNA, were taken up by cells *via* ligand-receptor specific interactions for their intended plasmid delivery.⁴⁰ However, any effect of photoactivation on potential enhancement of DNA delivery was not explored in these studies. Motivated by these findings, we decided to explore the potential of *sulfo*-pyro-PEI for preferred endosomal uptake (trap) and enhanced cytosolic delivery of DsiRNA (release) upon photoactivation.

We rationalized that non-sulfonated pyro-PEI complexed DsiRNA nanoparticles (pyro-PEI-NPs) are likely to be endocytosed but will primarily utilize a general mechanism involving enhanced ion influx and osmotically driven endosome disruption.^{41, 44, 46-48} In contrast, the endocytosed *sulfo*-pyro-PEI-NPs having a reduced number of available amines for protonation are predicted to mitigate ion influx and are unable to exploit osmotic swelling mechanisms for their intended cytosolic release. This restriction can be lifted by exploring a charge independent remote-strategy such as photoactivation of endosome-localized NPs enabling on-demand localized RNAi (Figure 1).

Sulfo-pyro-PEI that vary in their degree of sulfonation were examined for their ability to associate with the DsiRNA, their intracellular uptake, and the ability to enhance RNAi activity upon photoactivation. Interestingly, photoactivation of *sulfo*-pyro-PEI complexed-DsiRNA was found to be *essential* for gene silencing indicative of DsiRNA release into the cytosol in a regulated fashion. In contrast, *non*-sulfonated pyro-PEI complexed DsiRNA displayed gene silencing in the absence of photoactivation with no further increase in gene knock-down upon light treatments. This lack of photoactivation requirement for the *non*-sulfonated NPs can be interpreted as an alternate, non-specific, cytosolic DsiRNA release mechanism (potentially the proton sponge effect).⁴¹ Therefore, the photoactivation strategy described here presents a promising approach to facilitate regulated RNAi-induced gene silencing when using *sulfo*-pyro-PEI as the delivery agent. These photosensitizer-conjugated polyplexes provide a built-in engineered platform for directional activation and on demand RNAi with minimal side effects with translation potential in humans.

Methods

Materials

Nuclease and protease-free water was purchased from Quality Biological Inc. (Gaithersburg, MD). Cell titer blue reagent was obtained from Promega (Madison, WI, USA). Cell culture reagents and media were from Invitrogen (Grand Island, NY, USA). Nucleic acid sequences were purchased from Integrated DNA Technologies, Inc. (Coralville, Iowa, USA) (sequences

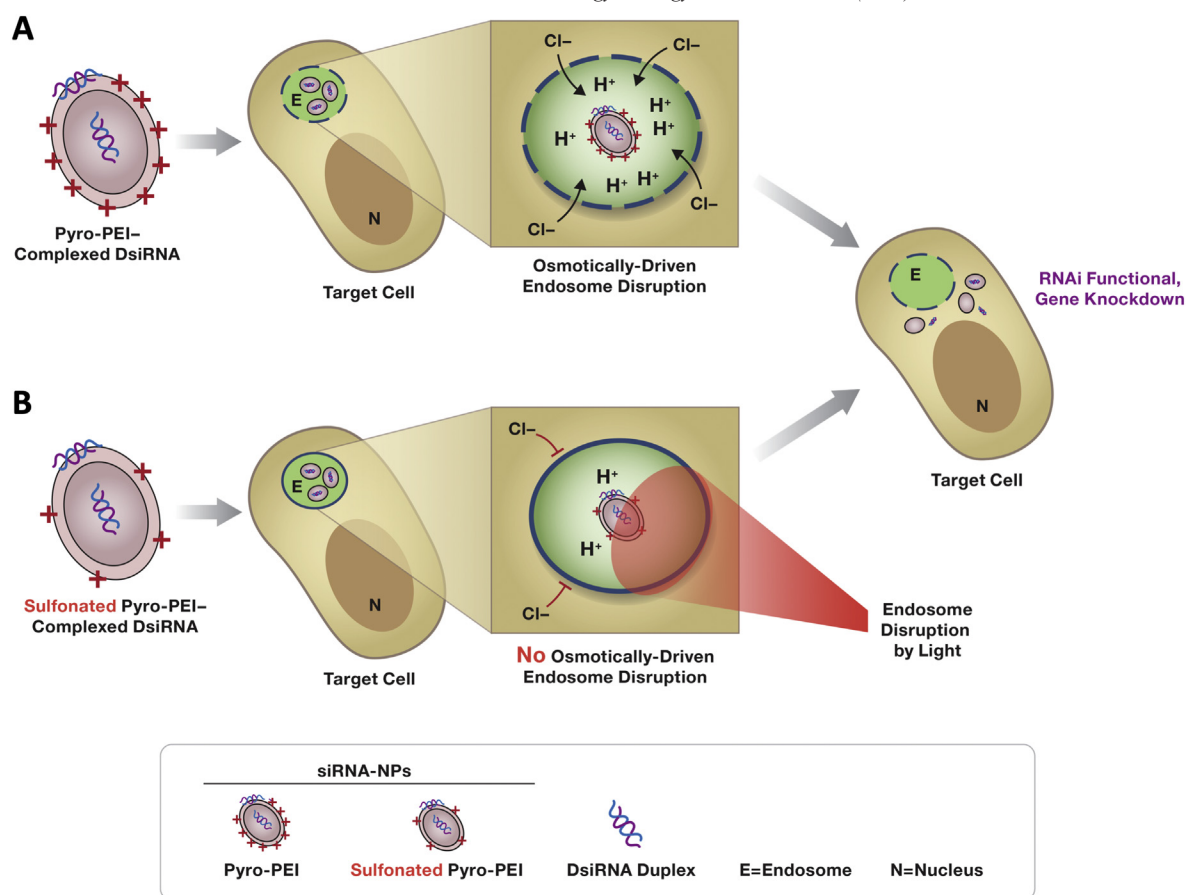


Figure 1. **Proposed hypothesis of selective siRNA delivery via photoactivation.** Pyro-PEI complexed siRNA-NPs are delivered into the target cell and accumulate in the endosomes. (A) Non-sulfonated pyro-PEI-NPs escape endosomes by way of the osmotic swelling mechanism. (B) The sulfo-pyro-PEI NPs on the other hand, remain trapped in the endosomes absent osmotic swelling. Photoactivation results in disruption of endosomal membrane, releasing NPs into the cytoplasm and initiating gene silencing (B, bottom panel).

provided in Supplemental section). RIPA lysis buffer and GAPDH mouse Mab (cat# sc-47724) were purchased from SANTA CRUZ Biotech., Inc. (Dallas, TX). Other antibodies for immunostaining assays were bought from ThermoFisher Scientific (Rockford, IL).

Preparation of pyro-PEI/nucleic acid complexes

Pyro-PEI and *sulfo*-pyro-PEI were synthesized and characterized as described⁴² (see supplemental material, Scheme 1, Figure S1). A dose response study was performed to optimize pyro-PEI/nucleic acid binding ratios. ATTO488-DNA duplexes were diluted in the assembly buffer at a concentration of 1 nmol/mL, and Pyro-PEI molecules were diluted in RNase/DNase free water as desired. A known concentration of DNA (3 pmol) was mixed with various amounts of the diluted pyro-PEI (containing 0-5 μ g), and samples were analyzed on a 2% agarose gel. DNA mobility was detected by image analysis using the Typhoon Trio variable mode imager (GE Healthcare) with a filter set of Ex/Em 488/532 nm (for ATTO488) and Ex/Em 488/670 nm (for pyro fluorescence).

For routine binding/uptake studies, pyro-PEI or *sulfo*-pyro-PEI were placed in 0.5 mL tubes and mixed with ATTO488-

DNA duplexes to a final DNA/pyro-PEI ratio of 1:165. These ATTO488-DNA-NPs were incubated for 30 min at room temperature, diluted 10-fold with phosphate buffered saline (PBS without $\text{Ca}^{2+}/\text{Mg}^{2+}$), and then used immediately for various experiments.

For gene silencing studies, anti-eGFP-DsiRNA-NPs or anti-PLK1-DsiRNA-NPs were prepared at a ratio of 10 nmol pyro-PEI or *sulfo*-pyro-PEI and 10 pmol DsiRNA in a volume of 50 μ L of the corresponding DsiRNA duplexes. Following incubations for 30 min at room temperature, the samples were diluted in 1 mL DMEM and were used immediately for gene silencing studies.

Sizing and zeta potential analysis of DsiRNA-NP complexes

DsiRNA-NPs were prepared using the anti-eGFP DsiRNA as described above and analyzed for their hydrodynamic size, particle concentration and zeta potential. For sizing, DsiRNA-NPs (10 μ L) were diluted in HEPES-buffered saline (HBS, pH 7.4) to a final volume of 400 μ L in 10 mM NaCl in a microcuvette. Dynamic light scattering measurements (12-24 acquisitions each) were acquired in triplicate using a Zeta Sizer Nano ZS (Malvern Instruments, MA). For zeta potential

measurements, DsiRNA-NPs or pyro-PEI samples without bound nucleic acids were diluted in 10 mM NaCl, in order to compare the effect of nucleic acid binding on reduction of overall charge.

Cell lines

Human breast cancer cells, MDA-MB-231 and green fluorescent protein expressing MDA-MB-231/GFP cells were procured from ATCC (Manassas, VA, USA) and Cell Biolabs Inc. (San Diego, CA, USA), respectively, and were maintained in DMEM supplemented with 10% FBS, 100 i.u./mL penicillin and 100 µg/mL streptomycin in 5% CO₂ at 37 °C.

Cell binding/uptake studies

ATTO488-DNA-NPs were incubated with MDA-MB-231 cells at a density of 10⁶/mL at desired temperatures for 2 h. Details of pyro-PEI/DNA ratios and exact incubation conditions are provided in the corresponding figure legends. Following incubations, cells were pelleted, washed, and analyzed for cell-associated ATTO488 fluorescence by flow cytometry.

Confocal microscopy

To visualize intracellular uptake of the NPs, MDA-MB-231 cells were plated on microwell-cutout petri dishes (0 mm glass cover slips) at a density of 2-3 × 10⁴ per well one day prior to binding/uptake assays. ATTO488-DNA-NPs diluted in 0.1 mL DMEM (0.5-1 pmol DNA) were added to the wells and incubations were continued for 4-6 h at 37 °C. Cells were washed with PBS-BSA (PBS containing 1% BSA) and fixed with 4% paraformaldehyde in PBS. Fixed cells were permeabilized using triton X100 (0.2% w/v in PBS, 0.1 mL per well), washed with PBS-BSA (×3, 1 mL each), and incubated with the early endosomal antigen 1 (EEA1) antibody (2 µg/mL in PBS-BSA) followed by incubations with rhodamine labeled goat antirabbit IgG (H + L) superclonal secondary Ab, essentially as described.⁴³ The nuclei were stained with DAPI according to manufacturer's recommendations. Imaging was performed using a Leica TCS SP8 microscope in laser scanning confocal mode using a 63× oil (1.4 N.A.) objective. The following laser lines were used: 405 nm (DAPI), 488 nm (ATTO488), and 552 nm (Rhodamine). Each image was taken with 0.5 µM z-steps.

Gene silencing studies

Reduction of eGFP expression was assessed by flow cytometry. MDA-MB-231/GFP cells, on 6-well clusters (10⁵ cells/well) were incubated with the corresponding anti-eGFP DsiRNA-NPs at low dose (1 nmol) or high dose (4 nmol) in 1 mL medium. Incubations were continued for 4-6 h at 37 °C. Cells were then harvested using the cell dissociation buffer, washed with HBSS⁺, resuspended in 0.2 mL buffer and divided into two equal parts. One part was treated with the 661 nm laser (0-15 min) and the other was an untreated control. The cells were diluted and placed in 24-well clusters and allowed to grow for 72 h. eGFP silencing was measured by flow cytometry.

For assessment of PLK1 silencing, non-GFP MDA-MB-231 cells suspended at 10⁶ cells/mL were incubated with anti-PLK1

DsiRNA-NPs using a ratio of 1 nmol NPs/10⁵ cells. Incubations were continued for 4-6 h at 37 °C. Cells were centrifuged, washed, resuspended in 0.5 mL HBSS⁺ and divided into two equal parts. One part was treated with the 661 nm laser (5 min) and the other was untreated. Following laser treatments, the cells were diluted in DMEM and placed in six-well clusters. Incubations were continued for 48 h at 37 °C. The cells were lysed using the RIPA buffer according to manufacturer's instructions. Lysates were analyzed by SDS-PAGE (4-12% bis/tris gel) and transferred to a nitrocellulose membrane (0.45 µm). PLK1 was identified using the anti-PLK1 mouse Mab (cat#13E8, ThermoFisher Scientific) and AlexaFluor-680-conjugated goat anti-mouse IgG (H + L) (cat# A21057, ThermoFisher Scientific). The membrane was imaged using the Amersham Typhoon 5 imager (GE Healthcare) with excitation/emission at 665 nm/720 nm.

Results

Description of variant pyro-PEI polymers

To develop photoactivatable RNAi therapeutics for localized delivery of DsiRNA, we explored a branched 10 kDa poly-ethylenimine polymer (PEI) covalently linked to the photosensitizing molecule pyro. Pyro was chosen for its desired spectral properties for future *in vivo* applications. Sulfonated pyro-PEI molecules (*sulfo*-pyro-PEI) differ in their overall positive charges due to the chemical modification of amines through introduction of sulfonate groups (Scheme 1, Figure S1). Previous studies show that selective sulfonation of pyro-PEI results in lowered cytotoxicity in CHO cells *in vitro*⁴².

In this study, we examined three pyro-PEIs: (i) non-sulfonated pyro-PEI (pyro-PEI), (ii) *sulfo*-pyro-PEI containing 6% amine modifications (pyro-s6-PEI), and (iii) *sulfo*-pyro-PEI containing 34% amine modifications (pyro-s34-PEI). The ability to generate reactive oxygen species after photoactivation (Figure S1) and the degree of photoactivation in the presence and absence of DsiRNA (Figure S2) was examined for pyro-PEIs differing in their extent of sulfonation. Ultimately, those pyro-PEIs with differing degrees of amine modification were investigated for their ability to promote conditional gene silencing by way of photo-triggered released of DsiRNA.

Sulfonation of pyro-PEI modulates binding with nucleic acid duplexes

A fluorescently labeled DNA duplex (ATTO488-DNA) was used to determine the effect of sulfonation on pyro-PEI binding affinity for nucleic acids. ATTO488-DNA duplexes incubated with various doses of the different pyro-PEI molecules were analyzed by agarose gel electrophoresis. A clear difference in binding affinity was observed for pyro-PEI and *sulfo*-pyro-PEI and correlated with the overall positive charge on the pyro-PEI, as expected (Figure 2, A). However, the differences in the dose response curves for the pyro-s6-PEI and pyro-s34-PEI were less significant. Based on binding data, DNA/pyro-PEI ratios of 1:165 were used for further cellular uptake studies.

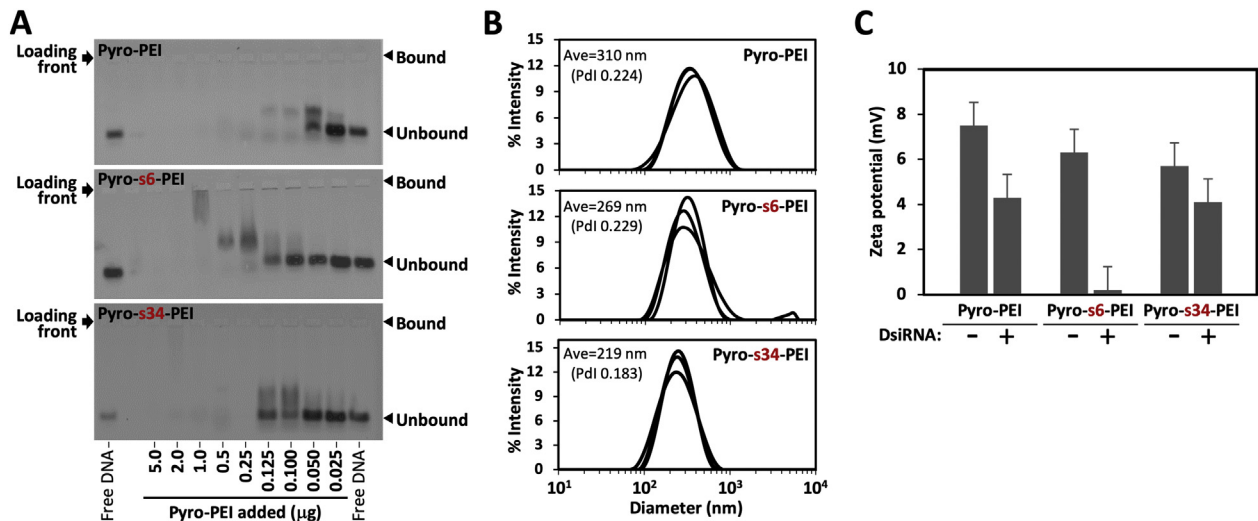


Figure 2. **Determination of PEI-nucleic acid interactions.** (A) Various amounts of pyro-PEI and *sulfo*-pyro-PEI bound to ATTO488-DNA duplexes were analyzed on a 2% agarose gel. PEI-bound DNA is retained in the wells and unbound DNA migrates in the gel as indicated by the mobility of the bands. (B) Hydrodynamic size of DsiRNA-NPs determined by dynamic light scattering. Graphs show average triplicate measurements. (C) Zeta potential was measured for PEI particles with and without bound DsiRNA.

Photoactivation treatments had no effects on the stability of ATTO488-DNA-NPs (supplemental section, Figure S3).

Next, the hydrodynamic size of anti-eGFP DsiRNA-NPs was determined by dynamic light scattering (DLS) measurements. Figure 2, B shows that the average diameter of pyro-PEI-DsiRNA-NPs decreased as the degree of sulfonation increased. Pyro-PEI NPs exhibited an average diameter of 310 nm (PDI 0.224), whereas pyro-s6-PEI and pyro-s34-PEI NPs had an average diameter of 269 nm (PDI 0.229) and 219 nm (PDI 0.183), respectively. Zeta potential values for pyro-PEI in absence of DsiRNA were $+7.5 \text{ mV} \pm 1.6$, whereas anti-eGFP DsiRNA-NPs showed a reduction in zeta potential ($+4.3 \text{ mV} \pm 0.8$) (Figure 2, C). Similar effects were observed for pyro-s34-PEI before ($+5.7 \text{ mV} \pm 2.5$) and after complexation with anti-eGFP DsiRNA duplex ($+4.1 \text{ mV} \pm 1.3$). In contrast, pyro-s6-PEI ($+6.3 \text{ mV} \pm 1.1$) after the DsiRNA binding showed a steep reduction in the zeta potential ($+0.2 \text{ mV} \pm 0.2$). This large drop in zeta potential for the pyro-s6-PEI NPs is a phenomenon we do not have a clear explanation for at this time.

Cellular uptake of pyro-PEI-complexed ATTO488-DNA

To monitor the effects of sulfonation of pyro-PEI on subsequent interactions with cells, we examined cellular uptake (representing the surface-bound and/or internalized NPs) of ATTO488-DNA-NPs with MDA-MB-231 cells under various conditions. Various concentrations of ATTO488-DNA duplexes (2.5, 5 or 10 pmol/ 10^6 cells) complexed with pyro-PEIs were incubated with MDA-MB-231 cells at 37 °C, and cell-associated fluorescence was determined by flow cytometry (Figure S4, A). The extent of ATTO488-DNA-NP binding varied linearly with concentration across the range of doses examined. Pyro-PEI complexed DNA displayed 1.5-2-fold greater binding to cells as compared to *sulfo*-pyro-PEI complexed DNA. However, differences in binding observed between pyro-s6 and pyro-s34-complexed DNA were relatively minor.

To further understand the nature of interactions between ATTO488-DNA-NPs and cells, we examined the effect of incubation temperature on binding, as the active endocytic mechanisms are known to be retarded at lower temperatures. Binding assays performed at a decreased temperature (4 °C) were compared with binding at 37 °C and clearly show that pyro-PEI-DNA complexes exhibit relatively higher cellular uptake compared to that for pyro-s34-PEI at both temperatures studied (Figure 3, A). Interestingly, these differences were more prominent at 4 °C, indicating that uptake of *sulfo*-pyro-PEI is more reliant on energy-dependent cellular processes (Figure 3, B). To further substantiate the observed temperature-dependent effects, we tested binding of ATTO488-DNA-NPs to cells across a range of temperatures (Figure 3, C). Enhanced binding of pyro-PEI complexed DNA was observed at all the temperatures tested, while pyro-s6-PEI and pyro-s34-PEI exhibited similar binding at each temperature. Taken together, cellular entry pathways for pyro- and *sulfo*-pyro-PEI complexed DNA duplexes are related to energy-dependent processes. Future detailed studies are warranted to map the exact intracellular uptake mechanism of these particles.

To gain further insight into the cellular uptake mechanisms of various pyro-PEI complexes, we examined the effects of trypsin treatment on the cell-associated ATTO488 fluorescence under various conditions (Figure S4, B). We observed that the trypsin sensitivity was similar for pyro-PEI and *sulfo*-pyro-PEIs. Most of the bound pyro-PEIs were cleaved by trypsin when binding was done at 4 °C, suggesting that at a lower temperature, the complexes remain surface bound. On the other hand, trypsin treatment resulted in only a partial decrease of ATTO488-DNA-NP fluorescence at 37 °C. These data suggest that the pyro-PEI and *sulfo*-pyro-PEI complexed nucleic acids are taken up *via* a similar mechanism. Again, detailed and thorough experiments are needed to further dissect out the exact cellular uptake patterns of these nanoparticles.

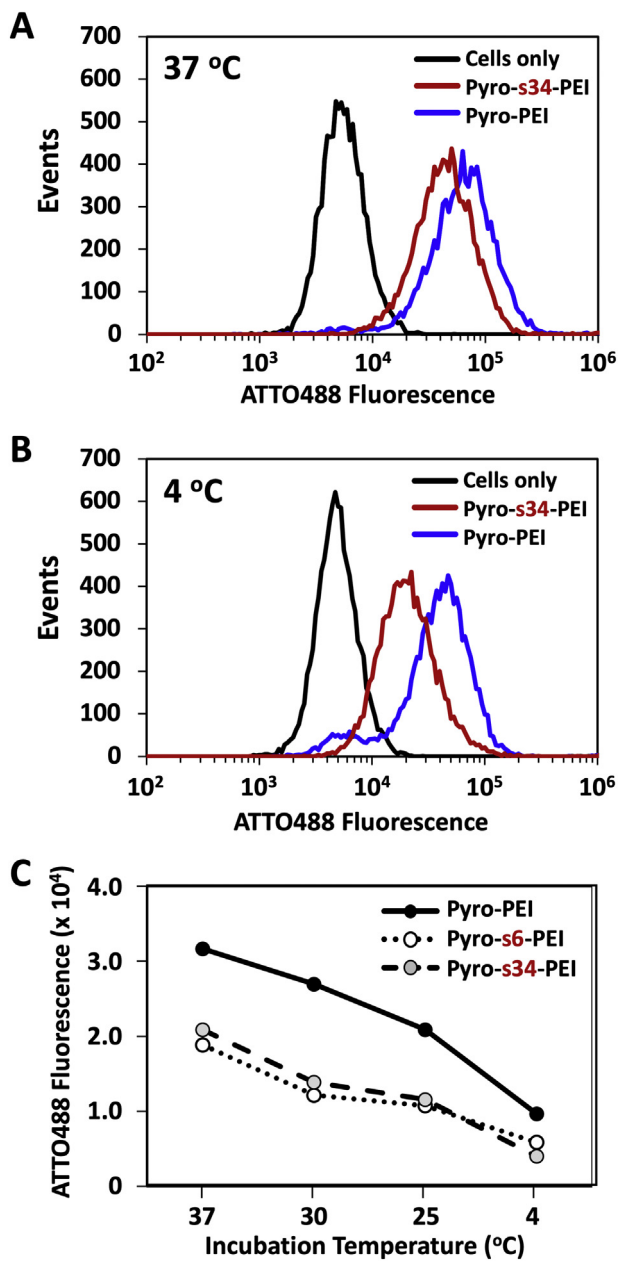


Figure 3. Uptake of ATTO488-DNA-NPs by MDA-MB-231 cells. MDA-MB-231 cells bound to ATTO488-DNA-NPs were analyzed by flow cytometry. Representative plots showing cellular fluorescence after uptake of ATTO488-DNA bound by pyro-PEI (blue curves) and *sulfo*-pyro-PEI (red curves) at (A) 37 °C and (B) 4 °C. Control cells are shown (black curves). (C) Relative binding of pyro-PEI, pyro-s6-PEI and pyro-s34-PEI ATTO488-DNA-NPs at various temperatures.

Sulfo-pyro-PEI-complexed DsiRNA promote eGFP silencing in MDA-MB-231/eGFP⁺ cells only upon photoactivation

Surface modification of nanoparticles is known to modulate interactions with negatively charged nucleic acids, as well as subsequent uptake by cells.³⁹ We speculated that sulfonated polymers may present an advantage for intracellular trafficking and sequestration into endosomes due to their inefficient protonation and impaired release (Figure 1). A dose-dependent study was

initially conducted to assess non-specific cellular toxicity of Pyro-PEI complexed DsiRNAs (Figure S5) prior to pursuing eGFP silencing studies. Anti-eGFP DsiRNA duplexes were complexed with various pyro-PEIs and gene silencing activity was measured in MDA-MB-231/eGFP⁺ cells. Clearly, only non-sulfonated pyro-PEI complexes mediated eGFP gene silencing in absence of laser treatment (Figure 4, A). However, this gene silencing was observed only at higher doses of the pyro-PEI (Figure 4, A, left panel, red curve as indicated by the arrow), but not at a lower dose (Figure 4, A, i, green curve). In contrast, *sulfo*-pyro-PEI complexed DsiRNA under identical conditions failed to show measurable eGFP silencing even when higher doses of the complexes were used (Figure 4, A, ii and iii, red curves). This lack of eGFP silencing was observed irrespective of the degree of sulfonation; neither pyro-s6-PEI (Figure 4, A, ii) nor pyro-s34-PEI (Figure 4, A, iii) complexed DsiRNA was able to downregulate eGFP under the experimental conditions examined.

Photoactivation rescues *sulfo*-pyro-PEI complexed DsiRNA mediated eGFP gene silencing in MDA-MB-231/eGFP⁺ cells

Various pyro-PEI-DsiRNA-NPs were bound to MDA-MB231/eGFP⁺ cells at two different doses for 4 h, after which cells were treated with a 661 nm laser for 0-15 min. Cells were then incubated at 37 °C for an additional 72 h after which eGFP expression levels were examined. When pyro-PEI was used for DsiRNA delivery, we did not observe any eGFP silencing at lower doses compared to control cells (Figure 4, B, i). At higher doses, a clear downregulation in eGFP levels was observed in samples that were not treated with the laser, and photoactivation resulted only in a slight enhancement of eGFP downregulation at this higher dose (Figure 4, B, iv). These data show that pyro-PEI complexed DsiRNA gene silencing occurs *via* an intracellular pathway that does not rely on the photoactivation of pyro-PEI.

However, when *sulfo*-pyro-PEIs were used, the results were quite different and interesting. We did not observe any eGFP gene downregulation for these samples in the absence of laser treatments, at either low or high doses. This lack of eGFP silencing in the absence of photoactivation was observed for both pyro-s6-PEI (Figure 4, B, ii & v) and pyro-s34-PEI (Figure 4, B, iii & vi) incubated cells. This observation contrasts with the pyro-PEI, where eGFP silencing was observed for high doses in absence of photoactivation (Figure 4, B, iv). Therefore, we conclude that the inability of *sulfo*-pyro-PEIs to promote eGFP silencing is not due to the limited DsiRNA in the cells.

Photoactivation of cells treated with *sulfo*-pyro-PEI complexes resulted in a clear induction of eGFP silencing, and this effect increased with longer duration of laser treatments. This effect of photoactivation-dependent silencing was observed for both *sulfo*-pyro-PEIs tested. eGFP downregulation occurred at both doses of the pyro-s6-PEI/DsiRNA complexes (Figure 4, B, ii & v), but the effect of photoactivation was more pronounced at higher doses of the pyro-s6-PEI. Cells incubated with pyro-s34-PEI/DsiRNA complexes clearly showed eGFP downregulation at both doses and silencing increased as a function of increased laser exposure. We observed that the efficiency of eGFP knock-down was similar between the low and high doses of the pyro-s34-PEI (Figure 4, B, iii & vi), and low dose pyro-s34-PEI

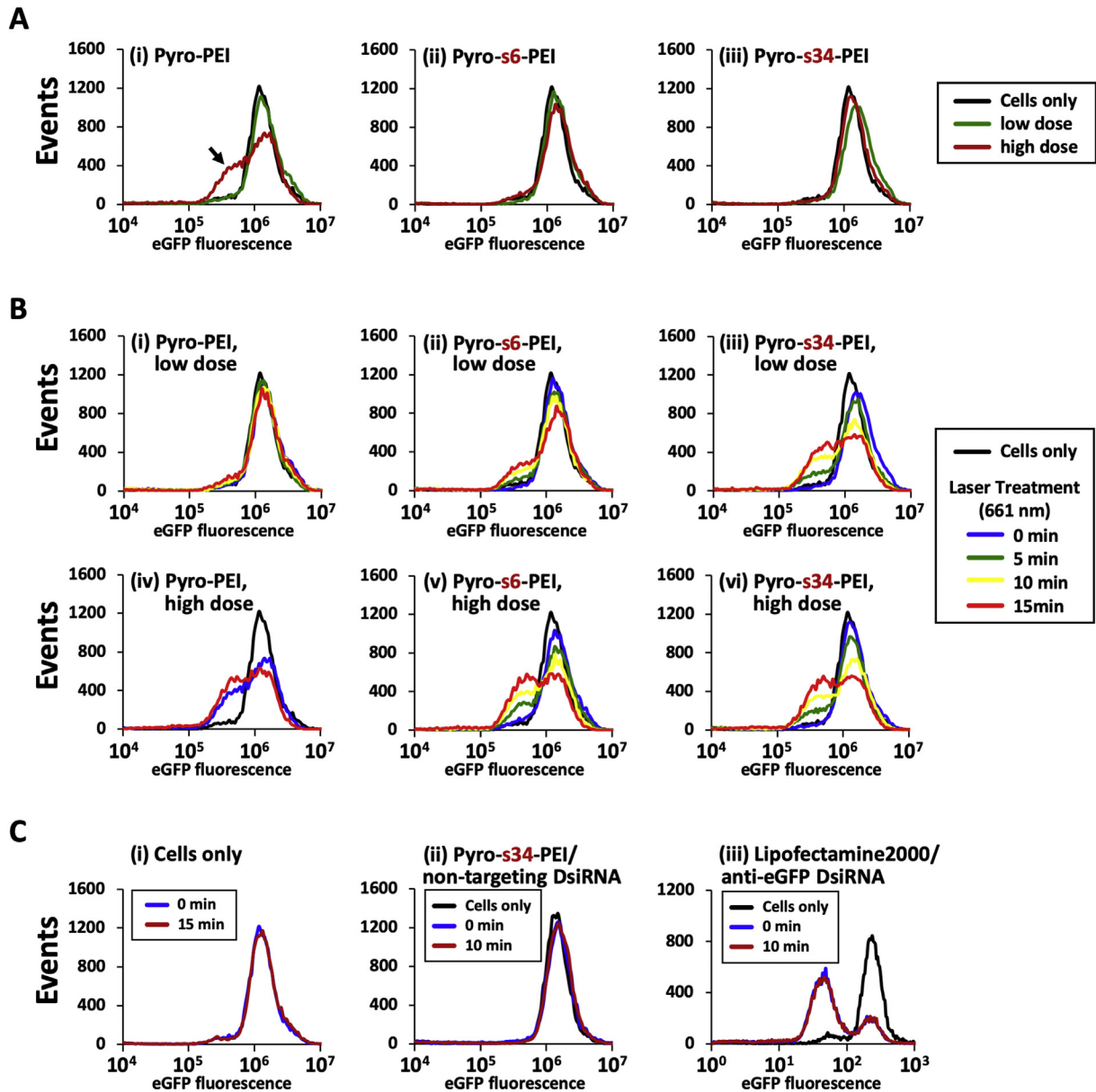


Figure 4. eGFP silencing in MDA-MB-231/eGFP⁺ cells by DsiRNA-NPs. DsiRNA-NPs at low dose (1 pmol RNA/1 nmol PEI per 10^5 cells) and high dose (4 pmol RNA/4 nmol PEI per 10^5 cells) concentrations were incubated with MDA-MB-231/eGFP⁺ cells on six-well clusters (10^5 cells per well). eGFP expression was measured by flow cytometry 72 h post-transfection. (A) eGFP fluorescence following transfection without laser treatment. (B) Cells were treated with a 661 nm laser 4 h following incubation with DsiRNA-NPs and eGFP fluorescence was measured post 72 h incubations. (C) Controls examining the effect of laser treatment (i) on non-transfected cells, (ii) following incubation with high-dose non-targeting DsiRNA-NPs and (iii) following anti-eGFP DsiRNA transfection using a non-photoreactive carrier.

showed markedly better silencing than low dose pyro-s6-PEI following photoactivation (Figure 4, B, ii & iii).

The possibility of any deleterious effects of laser treatment on eGFP expression was tested by treatment of the cells (i) in the absence of the pyro-PEI/DsiRNA NPs, (ii) incubations with scrambled DsiRNA/pyro-s34-PEI complexes (at high dose concentrations), and (iii) using lipofectamine as a transfection agent (Figure 4, C). Importantly, laser treatments of eGFP expressing cells alone, or pre-incubated with a non-targeting

sulfo-pyro-DsiRNA-NP, did not show any effects on eGFP expression. Additionally, laser treatments of cells transfected with anti-eGFP DsiRNA complexed with a non-photoreactive carrier had no impact on the extent of eGFP downregulation. These controls clearly show that the laser treatment conditions used in our experiments had no non-specific effects on eGFP expression or RNAi-based gene silencing. Taken together, sulfonated PEIs present a system for selective and on-demand DsiRNA delivery with minimal off-target effects.

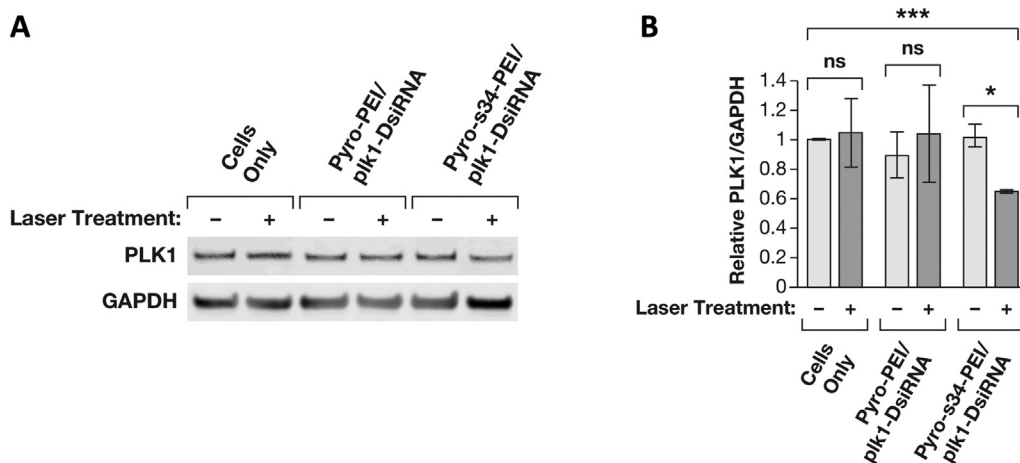


Figure 5. PLK1 downregulation in MDA-MB-231 cells by anti-PLK1 DsiRNA-NPs. MDA-MB-231 cell suspensions incubated with anti-PLK1 DsiRNA-NPs (at a low dose concentration corresponding to 1 pmol RNA per 10^5 cells) were treated with the laser for 5 min. Cells were lysed post 48-h incubations and PLK1 expression was determined by western blot analysis. GAPDH was used as a housekeeping gene control. The statistical significance of differences in PLK1 expression was determined from multiple experimental replicates by two-tailed Student's *t* test. *P* values are indicated as follows: n.s. (not significant) indicates $P > 0.05$; * indicates $P < 0.05$, *** indicates $P < 0.001$. Error bars represent \pm S.D.

Laser pretreatment downregulates PLK1 expression when anti-PLK1 DsiRNAs are delivered by sulfo-pyro-PEI NPs

Data presented above show that eGFP gene silencing can be selectively enhanced upon light treatment using the *sulfo*-pyro-PEI complexed DsiRNAs. Moreover, laser mediated restoration of eGFP silencing was clearly observed at lower doses of the NPs ($1 \text{ nmol NPs}/10^5 \text{ cells}$) where no gene silencing was observed for non-sulfonated NPs. Therefore, in our next set of experiments, we examined the effects of photoactivation on cellular expression of a protooncogene, PLK1, overexpressed in MDA-MB-231 cells,^{49,50} at low doses ($1 \text{ nmol NPs}/10^5 \text{ cells}$) of the NPs. PLK1 targeted RNAi was previously studied in clinical trials using a lipid-based formulation (TKM-080301) for the treatment of adrenocortical cancer⁵¹ and also in other related PLK1 RNAi *in vitro* and *in vivo* studies.^{50,52}

To examine the effect of photoactivation on PLK1 downregulation, MDA-MB-231 cells incubated with anti-PLK1-DsiRNA-NPs were treated with the laser and PLK1 expression was determined post 48-h incubations in the cell lysates. Results are presented in Figure 5. A statistically significant decrease in PLK1 expression was observed upon photoactivation in the cells incubated with *only sulfo*-pyro-PEI complexed anti-PLK1 DsiRNA (Figure 5, B). No obvious changes in PLK1 expression were observed in either control cells or in the cells incubated with non-sulfonated pyro-PEI complexed PLK1 siRNA, regardless of exposure to photoactivation. These results further confirm that the PLK1 downregulation occurs only upon photoactivation in samples incubated with *sulfo*-pyro-PEI-NPs. These results are in accordance with our observations on eGFP down-modulation (Figure 4, B). We noticed a slight increase in PLK1 expression upon laser treatments in control cells as well as in the cells incubated with non-sulfonated pyro-PEI NPs. However, these differences were found to be not statistically significant, confirming that laser treatment does not have any non-specific deleterious effects on gene expression. Taken together, these

results indicate the potential of selective photoactivation strategy for enhanced RNAi to treat cancer.

Sulfo-pyro-PEI bound ATTO488-DNA preferentially localizes in the endosomal compartments

Based on our data obtained from temperature dependence uptake and trypsin treatments, we concluded that pyro-PEI and *sulfo*-pyro-PEI molecules carry the nucleic acid to the cells presumably *via* similar pathways. The extent of cellular uptake by pyro-PEI NPs was increased presumably due to the overall higher positive charged residues on the surface of these NPs.

We examined intracellular distribution of these NPs relative to the endosomes by fluorescence microscopy. Here, we used EEA1, an endosomal marker to mark intracellular location in the cells (identified by rhodamine-labeled secondary antibody) and ATTO488 fluorescence to monitor the NPs. Results presented in Figure 6 show representative images for a given slice from confocal microscope images. These data suggest that *sulfo*-pyro-PEI NPs tend to preferentially localize in the vicinity of the endosomes whereas non-sulfonated particles appear randomly distributed. It is possible that the non-sulfonated PEI complexes are capable of escaping the endosomes without laser treatment and therefore do not show enhanced eGFP silencing upon photoactivation. A detailed study, subject to future investigations will be needed to map exact intracellular location of these NPs.

Discussion

Nanomedicine-based RNAi therapeutics are currently being explored and several formulations have paved their way to clinical trials.^{12, 19, 53} Site-specific delivery of the RNAi therapeutics as well as spatial and temporal release of the siRNA for its actions remains a challenge. In addition, unregulated siRNA release causes off-target effects.

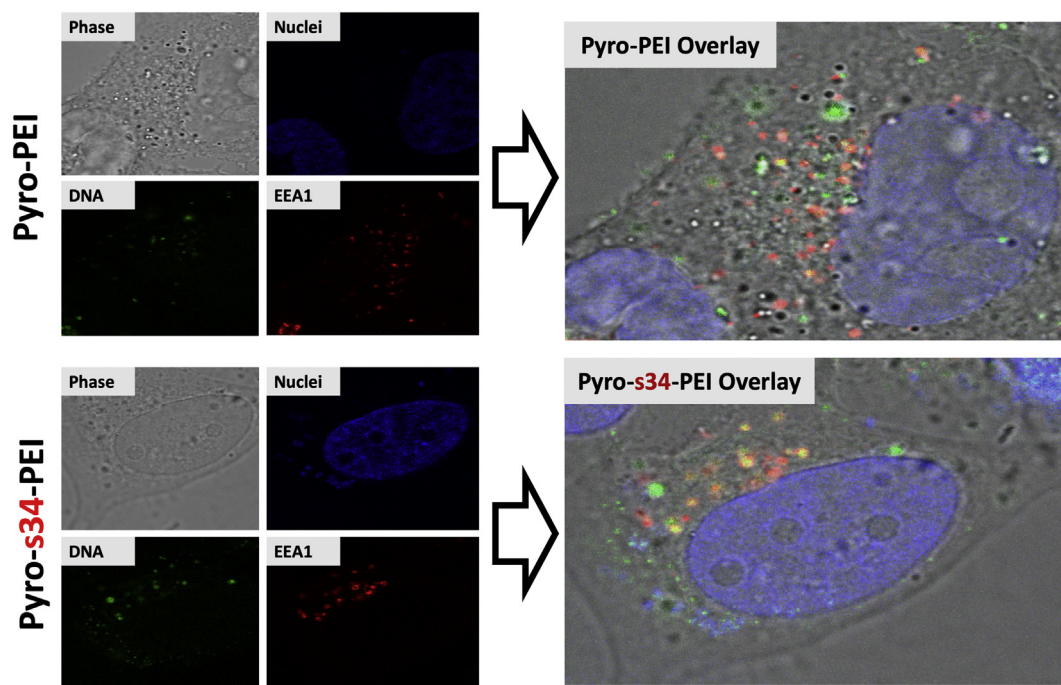


Figure 6. Visualization of cell-associated ATTO488-DNA-NPs by confocal microscopy. MDA-MB-231 cells on microwells were incubated with ATTO488-DNA-NPs, fixed, permeabilized and stained with EEA1 antibody as an early endosomal marker. Images for phase, DAPI (nuclei), ATTO488 (DNA) and rhodamine (EEA1) are shown on the left. An overlay of the images is shown on the right.

The inability of endocytosed siRNA-NPs to escape⁴⁵ into the cytoplasm, one of the major hurdles is an area of intense research.^{17,26,34,54,55} Several studies include pH, redox²⁹ or light activatable systems³²; photochemical internalization (PCI) being reported as a promising system with translational potential.^{31,56,57} The PCI approach relies on the delivery of the siRNA and the photosensitizer as separate entities with an assumption that both components will travel to the same intracellular compartment for their action. Our initial efforts to enhance cytosolic delivery of siRNA included a PDT molecule (HPPH) non-covalently partitioned into the positively charged DOTAP:DOPE liposomes. Although we observed an RNAi enhancement upon photoactivation, gene silencing prior to photoactivation was also clearly observed. Hence, this system failed to decrease off-target effects (unpublished data).

Polymer-based siRNA therapeutics have been developed^{58,59}; however, their utility as light-sensitive NPs has not yet been explored. Our PEI-based siRNA NPs contain a covalently linked tunable photosensitizing molecule (pyro) and hence present an advantage for intracellular site-specific co-delivery of the siRNA and the photoactivation molecule. Moreover, pyro can be activated by using wavelengths amenable for future applications *in vivo* (similar PDT molecules are currently used in the clinical settings). Sulfonated-Pyro PEIs also bear an advantage of reduced cellular toxicity of the carrier itself for their potential future clinical applications. Chemical synthesis of the pyro-conjugated PEIs involves simple steps with high yields providing the possibility of scale-up production of these molecules. *Sulfo*-pyro-PEIs only function upon light-activation

(no off-target effects) and show gene silencing at significantly lower doses of siRNA as compared to their non-sulfonated counterparts. Therefore, the photoactivation strategy described here presents a promising approach to facilitate regulated RNAi-induced gene silencing when using *sulfo*-pyro-PEI as the delivery agent. These photosensitizer-conjugated polyplexes provide a built-in engineered platform for directional activation and on demand RNAi with minimal side effects with translation potential in humans. Targeted RNAi therapies mediated through this technology are likely to improve cancer treatment due to the selective action of RNAi at the tumor site and are likely to have positive impact in the RNAi nanotherapeutics field.

Acknowledgments

This research was supported in part by the Intramural Research Program of the NIH, National Cancer Institute, Center for Cancer Research. This project has been funded in whole or in part with federal funds from the National Cancer Institute, National Institutes of Health, under contract HHSN261200800001E. The content of this publication does not necessarily reflect the views or policies of the Department of Health and Human Services, nor does mention of trade names, commercial products, or organizations imply endorsement by the U.S. Government.

This research was supported by the National Institutes of Health (R01EB017270 and DP5OD017898) the National Science Foundation (1555220) and the University at Buffalo Clinical and Translational Science Institute.

Appendix A. Supplementary data

Supplementary data to this article can be found online at <https://doi.org/10.1016/j.nano.2020.102176>.

References

1. Fire A, Xu S, Montgomery MK, Kostas SA, Driver SE, Mello CC. Potent and specific genetic interference by double-stranded RNA in *Caenorhabditis elegans*. *Nature* 1998;**391**(6669):806-11.
2. Rana TM. Illuminating the silence: understanding the structure and function of small RNAs. *Nat Rev Mol Cell Biol* 2007;**8**(1):23-36.
3. Jeang KT. RNAi in the regulation of mammalian viral infections. *BMC Biol* 2012;**10**:58.
4. Pai SI, Lin YY, Macaes B, Meneshian A, Hung CF, Wu TC. Prospects of RNA interference therapy for cancer. *Gene Ther* 2006;**13**(6):464-77.
5. Koenig O, Walker T, Perle N, Zech A, Neumann B, Schlensak C, et al. New aspects of gene-silencing for the treatment of cardiovascular diseases. *Pharmaceuticals (Basel)* 2013;**6**(7):881-914.
6. Kaiser PK, Symons RC, Shah SM, Quinlan EJ, Tabandeh H, Do DV, et al. SiRNA-027 Study, I., RNAi-based treatment for neovascular age-related macular degeneration by SiRNA-027. *Am J Ophthalmol* 2010;**150**(1):33-9 e2.
7. Guzman-Aranguiz A, Loma P, Pintor J. Small-interfering RNAs (siRNAs) as a promising tool for ocular therapy. *Br J Pharmacol* 2013;**170**(4):730-47.
8. Kanasty R, Dorkin JR, Vegas A, Anderson D. Delivery materials for siRNA therapeutics. *Nat Mater* 2013;**12**(11):967-77.
9. Ozpolat B, Sood AK, Lopez-Berestein G. Nanomedicine based approaches for the delivery of siRNA in cancer. *J Intern Med* 2010;**267**(1):44-53.
10. Musacchio, T.; Torchilin, V. P., siRNA delivery: from basics to therapeutic applications. *Front Biosci (Landmark Ed)* 2013, **18**, 58–79.
11. Bobbin ML, Rossi JJ. RNA interference (RNAi)-based therapeutics: delivering on the promise? *Annu Rev Pharmacol Toxicol* 2016;**56**:103-22.
12. Ozcan G, Ozpolat B, Coleman RL, Sood AK, Lopez-Berestein G. Preclinical and clinical development of siRNA-based therapeutics. *Adv Drug Deliv Rev* 2015;**87**:108-19.
13. Kim DH, Behlke MA, Rose SD, Chang MS, Choi S, Rossi JJ. Synthetic dsRNA dicer substrates enhance RNAi potency and efficacy. *Nat Biotechnol* 2005;**23**(2):222-6.
14. Rose SD, Kim DH, Amarzguoui M, Heidel JD, Collingwood MA, Davis ME, et al. Functional polarity is introduced by dicer processing of short substrate RNAs. *Nucleic Acids Res* 2005;**33**(13):4140-56.
15. Guo P. The emerging field of RNA nanotechnology. *Nat Nanotechnol* 2010;**5**(12):833-42.
16. Afonin KA, Kasprzak WK, Bindewald E, Kireeva M, Viard M, Kashlev M, et al. In silico design and enzymatic synthesis of functional RNA nanoparticles. *Acc Chem Res* 2014;**47**(6):1731-41.
17. Parlea L, Puri A, Kasprzak W, Bindewald E, Zakrevsky P, Satterwhite E, et al. Cellular delivery of RNA nanoparticles. *ACS Comb Sci* 2016;**18**(9):527-47.
18. Shu Y, Pi F, Sharma A, Rajabi M, Haque F, Shu D, et al. Stable RNA nanoparticles as potential new generation drugs for cancer therapy. *Adv Drug Deliv Rev* 2014;**66**:74-89.
19. Sridharan K, Gogtay NJ. Therapeutic nucleic acids: current clinical status. *Br J Clin Pharmacol* 2016;**82**(3):659-72.
20. Yousefi A, Storm G, Schiffelers R, Mastrobattista E. Trends in polymeric delivery of nucleic acids to tumors. *Journal of controlled release : official journal of the Controlled Release Society* 2013;**170**(2):209-18.
21. Mittal A, Chitkara D. Structural modifications in polymeric micelles to impart multifunctionality for improved drug delivery. *Ther Deliv* 2016;**7**(2):73-87.
22. Wagner E. Polymers for nucleic acid transfer—an overview. *Adv Genet* 2014;**88**:231-61.
23. Neuberger P, Kichler A. Recent developments in nucleic acid delivery with polyethylenimines. *Adv Genet* 2014;**88**:263-88.
24. Jiang Y, Hardie J, Liu Y, Ray M, Luo X, Das R, et al. Nanocapsule-mediated cytosolic siRNA delivery for anti-inflammatory treatment. *Journal of controlled release : official journal of the Controlled Release Society* 2018;**283**:235-40.
25. Ding Y, Wang Y, Zhou J, Gu X, Wang W, Liu C, et al. Direct cytosolic siRNA delivery by reconstituted high density lipoprotein for target-specific therapy of tumor angiogenesis. *Biomaterials* 2014;**35**(25):7214-27.
26. Salzano G, Costa DF, Torchilin VP. siRNA delivery by stimuli-sensitive nanocarriers. *Curr Pharm Des* 2015;**21**(31):4566-73.
27. Krupa A, Fol M, Rahman M, Stokes KY, Florence JM, Leskov IL, et al. Silencing Bruton's tyrosine kinase in alveolar neutrophils protects mice from LPS/immune complex-induced acute lung injury. *American journal of physiology. Lung cellular and molecular physiology* 2014;**307**(6):L435-48.
28. Wittrup A, Ai A, Liu X, Hamar P, Trifonova R, Charisse K, et al. Visualizing lipid-formulated siRNA release from endosomes and target gene knockdown. *Nat Biotechnol* 2015;**33**(8):870-6.
29. Chen G, Wang Y, Xie R, Gong S. Tumor-targeted pH/redox dual-sensitive unimolecular nanoparticles for efficient siRNA delivery. *Journal of controlled release : official journal of the Controlled Release Society* 2017;**259**:105-14.
30. Yang Y, Yang Y, Xie X, Xu X, Xia X, Wang H, et al. Dual stimulus of hyperthermia and intracellular redox environment triggered release of siRNA for tumor-specific therapy. *Int J Pharm* 2016;**506**(1–2):158-73.
31. Oliveira S, Hogset A, Storm G, Schiffelers RM. Delivery of siRNA to the target cell cytoplasm: photochemical internalization facilitates endosomal escape and improves silencing efficiency, in vitro and in vivo. *Curr Pharm Des* 2008;**14**(34):3686-97.
32. Matsushita-Ishiodori Y, Ohtsuki T. Photoinduced RNA interference. *Acc Chem Res* 2012;**45**(7):1039-47.
33. Zhu, L.; Torchilin, V. P., Stimulus-responsive nanopreparations for tumor targeting. *Integr. Biol. (Camb.)* **2013**, *5* (1), 96–107.
34. Ganta S, Devalapally H, Shahiwala A, Amiji M. A review of stimuli-responsive nanocarriers for drug and gene delivery. *J Control Release* 2008;**126**(3):187-204.
35. Yavlovich A, Smith B, Gupta K, Blumenthal R, Puri A. Light-sensitive lipid-based nanoparticles for drug delivery: design principles and future considerations for biological applications. *Mol Membr Biol* 2010;**27**(7):364-81.
36. Puri A. Phototriggerable liposomes: current research and future perspectives. *Pharmaceutics* 2013;**6**(1):1-25.
37. Voigt J, Christensen J, Shastri VP. Differential uptake of nanoparticles by endothelial cells through polyelectrolytes with affinity for caveolae. *Proc Natl Acad Sci U S A* 2014;**111**(8):2942-7.
38. Varki A. Selectin ligands. *Proc Natl Acad Sci* 1994;**91**(16):7390-7.
39. Chitgupi U, Zhang Y, Lo CY, Shao S, Song W, Geng J, et al. Sulfonated polyethylenimine for photosensitizer conjugation and targeting. *Bioconjug Chem* 2015;**26**(8):1633-9.
40. Chitgupi U, Li Y, Chen M, Shao S, Beitelshes M, Tan MJ, et al. Bimodal targeting using sulfonated, mannosylated PEI for combined gene delivery and photodynamic therapy. *Photochem Photobiol* 2017;**93**(2):600-8.
41. Vermeulen LMP, Brans T, Samal SK, Dubruiel P, Demeester J, De Smedt SC, et al. Endosomal size and membrane leakiness influence proton sponge-based rupture of endosomal vesicles. *ACS Nano* 2018;**12**(3):2332-45.
42. Chitgupi U, Zhang Y, Lo CY, Shao S, Song W, Geng J, et al. Sulfonated polyethylenimine for photosensitizer conjugation and targeting. *Bioconjug Chem* 2015;**26**(8):1633-9.
43. Gupta K, Mattingly SJ, Knipp RJ, Afonin KA, Viard M, Bergman JT, et al. Oxime ether lipids containing hydroxylated head groups are more

- superior siRNA delivery agents than their nonhydroxylated counterparts. *Nanomedicine (London, England)* 2015;**10**(18):2805-18.
44. Elkin SR, Lakoduk AM, Schmid SL. Endocytic pathways and endosomal trafficking: a primer. *Wiener Medizinische Wochenschrift* 2016;**166**(7):196-204.
 45. Shete HK, Prabhu RH, Patravale VB. Endosomal escape: a bottleneck in intracellular delivery. *J Nanosci Nanotechnol* 2014;**14**(1):460-74.
 46. Bodenstein TM, Seftor RE, Seftor EA, Khalkhali-Ellis Z, Samii NA, Monarrez JC, et al. Internalization by multiple endocytic pathways and lysosomal processing impact mspn-based therapeutics. *Mol Cancer Res* 2014;**12**(10):1480-91.
 47. Yamaguchi H, Takeo Y, Yoshida S, Kouchi Z, Nakamura Y, Fukami K. Lipid rafts and caveolin-1 are required for invadopodia formation and extracellular matrix degradation by human breast cancer cells. *Cancer Res* 2009;**69**(22):8594-602.
 48. Anderson RG. The caveolae membrane system. *Annu Rev Biochem* 1998;**67**:199-225.
 49. Hattori Y, Kikuchi T, Ozaki KI, Onishi H. Evaluation of in vitro and in vivo therapeutic antitumor efficacy of transduction of polo-like kinase 1 and heat shock transcription factor 1 small interfering RNA. *Exp Ther Med* 2017;**14**(5):4300-6.
 50. Spankuch B, Kurunci-Csacsco E, Kaufmann M, Strebhardt K. Rational combinations of siRNAs targeting Plk1 with breast cancer drugs. *Oncogene* 2007;**26**(39):5793-807.
 51. Demeure MJ, Armaghany T, Ejadi S, Ramanathan RK, Elfiky A, Strosberg JR, et al. A phase I/II study of TKM-080301, a PLK1-targeted RNAi in patients with adrenocortical cancer (ACC). *Journal of Clinical Oncology* 2016;**34**(15_suppl):2547.
 52. Malhotra M, Tomaro-Duchesneau C, Saha S, Prakash S. Systemic siRNA delivery via peptide-tagged polymeric nanoparticles, targeting PLK1 gene in a mouse xenograft model of colorectal cancer. *International journal of biomaterials* 2013;**2013**:252531.
 53. Guo W, Chen W, Yu W, Huang W, Deng W. Small interfering RNA-based molecular therapy of cancers. *Chin J Cancer* 2013;**32**(9):488-93.
 54. Endoh T, Sisido M, Ohtsuki T. Spatial regulation of specific gene expression through photoactivation of RNAi. *Journal of controlled release : official journal of the Controlled Release Society* 2009;**137**(3):241-5.
 55. Fan B, Kang L, Chen L, Sun P, Jin M, Wang Q, et al. Systemic siRNA delivery with a dual pH-responsive and tumor-targeted nanovector for inhibiting tumor growth and spontaneous metastasis in orthotopic murine model of breast carcinoma. *Theranostics* 2017;**7**(2):357-76.
 56. Zhu K, Liu G, Hu J, Liu S. Near-infrared light-activated photochemical internalization of reduction-responsive polyprodrug vesicles for synergistic photodynamic therapy and chemotherapy. *Biomacromolecules* 2017;**18**(8):2571-82.
 57. Berg K, Weyergang A, Prasmickaite L, Bonsted A, Hogset A, Strand MT, et al. Photochemical internalization (PCI): a technology for drug delivery. *Methods in molecular biology (Clifton, NJ)* 2010;**635**:133-45.
 58. Shen ZL, Xia YQ, Yang QS, Tian WD, Chen K, Ma YQ. Polymer-nucleic acid interactions. *Topics in current chemistry (Cham)* 2017;**375**(2):44.
 59. Reynolds N, Dearnley M, Hinton TM. Polymers in the delivery of siRNA for the treatment of virus infections. *Topics in current chemistry (Cham)* 2017;**375**(2):38.